Estimating Patient Specific Templates for Pre-operative and Follow-Up Brain Tumor Registration

Dongjin Kwon, Ke Zeng, Michel Bilello, and Christos Davatzikos

Center for Biomedical Image Computing and Analytics,
University of Pennsylvania, Philadelphia, PA, USA

Abstract. Deformable registration between pre-operative and follow-up scans of glioma patients is important since it allows us to map post-operative longitudinal progression of the tumor onto baseline scans, thus, to develop predictive models of tumor infiltration and recurrence. This task is very challenging due to large deformations, missing correspondences, and inconsistent intensity profiles between the scans. Here, we propose a new method that combines registration with estimation of patient specific templates. These templates, built from pre-operative and follow-up scans along with a set of healthy brain scans, approximate the patient's brain anatomy before tumor development. Such estimation provides additional cues for missing correspondences as well as inconsistent intensity profiles, and therefore guides better registration on pathological regions. Together with our symmetric registration framework initialized by joint segmentation-registration using a tumor growth model, we are also able to estimate large deformations between the scans effectively. We apply our method to the scans of 24 glioma patients, achieving the best performance among compared registration methods.

1 Introduction

Glioblastoma is a very aggressive brain tumor, which infiltrates well beyond visible tumor boundaries. Finding imaging signatures that can predict tumor infiltration and subsequent tumor recurrence is very important in treatment of brain gliomas, as it could potentially affect treatment decisions at baseline patient evaluations [1]. This necessitates the development of accurate deformable registration methods that establish spatial correspondences between the pre-operative and follow-up brain scans, which allow follow-up information to be mapped onto baseline scans and elucidate imaging signatures for more aggressively infiltrated tissue, and accordingly inform pre-surgical planning procedures. This process must account for large deformations present in the pre-operative scan due to mass effect by tumor, as well as in the follow-up scan after tumor resection and tissue relaxation. Moreover, edema and tumor infiltration further confound the anatomy around the tumor. Even though the scans come from the same patient, this intra-subject registration task is very challenging due to these large deformations, missing correspondences, and inconsistent intensity profiles between the scans.

N. Navab et al. (Eds.): MICCAI 2015, Part II, LNCS 9350, pp. 222–229, 2015.
DOI: 10.1007/978-3-319-24571-3_27

Most existing registration methods exclude the pathological regions to deal with missing correspondences [9,3,7]. The concept of guiding registration via segmentation is used by methods performing intra-subject registration of scans capturing an evolving tumor [7] or inter-subject registration of scans for healthy brains and the one with pathology [9,3]. However, it is difficult to estimate large deformations on brain tumors by simply excluding the pathology. To take account of pathological regions, there exist different approaches performing inter-subject registrations by inpainting pathological regions [11] or estimating low-rank images iteratively [6]. For intra-subject registrations, Kwon et al. [4], design a registration framework specific to the pre-operative and post-recurrence scans. This method estimates a patient specific probabilistic prior aligned with the follow-up scan and jointly segments and registers with the pre-operative scan by growing a tumor from the location of resection. However, pathological regions, such as edema, are excluded in the matching cost, as one could not establish correspondences for these regions. As a result, the deformation field is solely determined through associated displacements of surrounding tissues via regularization, a procedure that could potentially compromise registration accuracy.

In this paper, we propose a new method combining registration and estimation of patient specific templates for pre-operative and follow-up brain tumor scans. As the follow-up scan is freed from an often huge mass effect and intense peritumoral edema by surgical resection of the glioma, we assume that the follow-up scans contain enough information for us to estimate the patient's brain anatomy before tumor development, using informative prior knowledge of brain structure provided by a set of healthy brain scans. Such estimation could be propagated to the pre-operative space, given the reasonable mapping between scans. Our method estimates this mapping by registering pre-operative and follow-up scans by excluding pathological regions estimated by [4] in calculating matching cost. After estimating patient specific templates on both scans, pathological regions that have been confidently estimated no longer need to be masked out in the matching cost, providing extra information to the registration process in order to identify correspondences. Note that we use the term "inpainting" for our estimation of patient specific templates, considering the similarities of the task that fills missing areas using prior knowledge.

In the rest of this paper, we describe the segmentation methods for pre-operative and follow-up brain tumor scans in Sec. 2 and our combined registration and inpainting framework in Sec. 3. In Sec. 4, we present our quantitative and qualitative evaluations and conclude the paper in Sec. 5.

2 Segmentation of Pre-operative and Follow-Up Scans

In this section, we estimate posterior probabilities of the pre-operative (baseline) scan B and follow-up scan F and the initial mapping between B and F based on [4]. As F is usually closer to the normal anatomy by the surgical resection of the glioma, we firstly segment F by aligning an atlas of the healthy population to F. Then we segment B and simultaneously register B and F by simulating

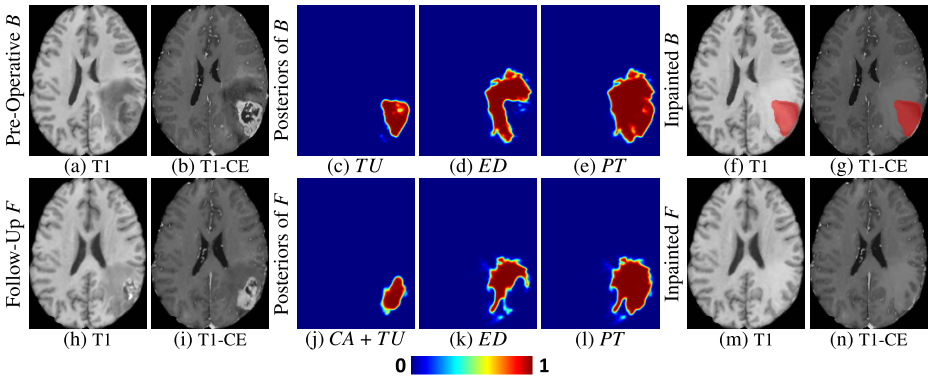

Fig. 1. An example of posteriors and estimated patient specific templates by inpainting pathological regions. For the pre-operative scan B, we show subject scans in (a)-(b), posteriors for tumor (TU), edema (ED), and pathological regions (PT) in (c)-(e), patient specific templates in (f)-(g). In (f)-(g), tumor regions are masked as they don't belong to the normal anatomy. For the follow-up scan F, we show subject scans in (h)-(i), posteriors of cavity (CA) with tumor, edema, and pathological regions in (j)-(l), patient specific templates in (m)-(n).

tumor growths on this aligned atlas. We denote by '$\mathcal{T}_t|\mathbf{x}$' the tissue type being t at voxel $\mathbf{x}$, namely '$\mathcal{T} = t|\mathbf{x}$'. The atlas p_A is defined as a set of probability maps $p_A(\mathcal{T}_t|\mathbf{x})$ for white matter (WM), gray matter (GM), and cerebrospinal fluid (CSF), i.e. $t \in \{WM, GM, CSF\}$.

For segmenting F, we define spatial probabilities $p_F(\mathcal{T}_t|\mathbf{x})$ of F for each tissue type t by combining p_A with a simple model for pathology described in [4]. This model generates a spatial probability for pathological regions, such as cavity (t=CA), tumor recurrences (t=TR) and edema (t=ED), using the generalized logistic function given the approximated center point and radius for each region of the cavity or tumor recurrence. We then estimate the mapping $\boldsymbol{h}^*_F$ and the posterior probabilities $p_F(\mathcal{T}_t|F, \mathbf{x})$ by registering $p_F(\mathcal{T}_t|\mathbf{x})$ with F via the expectation-maximization (EM) algorithm. We show an example of posteriors for pathological regions in Fig. 1 (j)-(l).

To segment B and estimate the initial mapping between B and F, we apply a joint segmentation-registration method [5] on the atlas aligned with F, defined as $p_S(\mathcal{T}_t|\mathbf{x}) \triangleq p_A(\mathcal{T}_t|\boldsymbol{h}^*_F(\mathbf{x}))$. This method generates the spatial probabilities of tumor (t=TU) and edema (t=ED) by applying a tumor growth model on the space of F and combine them with p_S to define spatial probabilities $p_B(\mathcal{T}_t|\mathbf{x})$ of B. Similar to the method for F, it estimates the mapping $\boldsymbol{h}^*_B$ and the posterior probabilities $p_B(\mathcal{T}_t|B, \mathbf{x})$ by registering $p_B(\mathcal{T}_t|\mathbf{x})$ with B via the EM algorithm. Then the initial mapping between B and F, denoted by $\boldsymbol{f}^0_{BF}$, is obtained by concatenating $\boldsymbol{h}^*_B$ and the mapping $\mathbf{u}^*$ representing the mass effect from the tumor growth model. The mapping $\boldsymbol{f}^0_{BF}$ approximates the mapping between B and F as the spatial probabilities p_S having smoothed anatomical information is used for the alignment instead of F. We show an example of posteriors for pathological regions in Fig. 1 (c)-(e).

3 Combined Registration and Inpainting Framework

Having defined the posterior probabilities p_B and p_F and the initial mapping $\boldsymbol{f}^0_{BF}$, we now describe our combined registration and inpainting framework to obtain final mapping $\boldsymbol{f}_{BF}$. To determine the large deformation reliably, we apply a symmetric registration scheme to match both scans to a center coordinate system Ω_C. Then we split the mapping $\boldsymbol{f}_{BF}$ into a mapping from Ω_C to Ω_B, $\boldsymbol{f}_{CB}$ and a mapping from Ω_C to Ω_F, $\boldsymbol{f}_{CF}$ as follows:

$$\boldsymbol{f}_{BF} \triangleq \boldsymbol{f}_{CF} \circ (\boldsymbol{f}_{CB})^{-1}, \tag{1}$$

where "$\circ$" concatenates two mappings. For registration, we model an energy function $E(\cdot)$ composed of a correspondence term E_C, a pathology term E_P, and a smoothness term E_S and estimate optimal mappings $\{\boldsymbol{f}^*_{CB}, \boldsymbol{f}^*_{CF}\}$ by minimizing $E(\cdot)$:

$$\{\boldsymbol{f}^*_{CB}, \boldsymbol{f}^*_{CF}\} = \arg \min_{\boldsymbol{f}_{CB}, \boldsymbol{f}_{CF}} E(\boldsymbol{f}_{CB}, \boldsymbol{f}_{CF}; B, F, p_B, p_F) \, . \tag{2}$$

Then we calculate optimal mappings $\boldsymbol{f}^*_{BF}$ and $\boldsymbol{f}^*_{FB} \triangleq (\boldsymbol{f}^*_{BF})^{-1}$ using (1). Our framework firstly estimates the optimal mappings while masking out correspondences on the pathological regions using p_B and p_F, then we estimate patient specific templates by inpainting pathological regions of B and F using aligned healthy brain sets. After estimating patient specific templates, we update the optimal mappings by including correspondences on the pathological regions. The remainder of this section describes our inpainting method and then our energy function in detail.

To inpaint pathological regions of F, let $\mathcal{I}_F = \{I_n\}_{n=1}^N$ be a set of N healthy brain templates aligned with F by applying a nonrigid registration method [2] (with the histogram matching) to each pair of I_n and F with the foreground mask computed using p_F. Based on our observation that F is closer to the normal anatomy compared with B, we register healthy brain templates on F rather than B. We also provide the foreground mask computed using p_F. For each voxel $\mathbf{x} \in \Omega_F$ having non-zero posteriors of pathological regions ($t \in \{CA, TR, ED\}$), we find the index of the best matching template $n^*_F(\mathbf{x})$ by minimizing patch-based distances between I_n and F and between I_n and $B \circ \boldsymbol{f}^*_{FB}$ (aligning B into F).

$$n^*_F(\mathbf{x}) = \arg \min_n D_{SSD}(F, I_n, \mathbf{x}) + \alpha \cdot D_{SSD}(B \circ \boldsymbol{f}^*_{FB}, I_n, \mathbf{x}) \, , \tag{3}$$

where $D_{SSD}(\cdot, \cdot, \mathbf{x})$ is the sum of squared distance (SSD) between patches of two input scans centered on $\mathbf{x}$. After estimating $n^*_F(\mathbf{x})$ for pathological regions, we synthesize these regions of F by simply averaging the best matching patches while other advanced methods could also be applied [10]. To inpaint B, we align the set of healthy brain templates into B by applying $\boldsymbol{f}^*_{BF}$ to each template, i.e. $\mathcal{I}_B = \{I_n \circ \boldsymbol{f}^*_{BF}\}_{n=1}^N$. Similar to the case of F, the index of the best matching template $n^*_B(\mathbf{x})$ is estimated for each voxel having non-zero posteriors of pathological regions ($t \in \{TU, ED\}$) by

$$n^*_B(\mathbf{x}) = \arg \min_n D_{SSD}(B, I_n \circ \boldsymbol{f}^*_{BF}, \mathbf{x}) + \alpha \cdot D_{SSD}(F \circ \boldsymbol{f}^*_{BF}, I_n \circ \boldsymbol{f}^*_{BF}, \mathbf{x}) \, . \tag{4}$$

In (3) and (4), the best matching patch would be consistent with both scans when $\alpha > 0$. We iterate the estimation of the index $\{n_F^*, n_B^*\}$ by applying synthesized scans F and B on the previous iteration in (3) and (4). On the first iteration, we set $\alpha = 0$ and compute D_{SSD} only on the healthy regions (when posteriors of pathological regions are zero). If there exists limited healthy brain regions in the patch, we adaptively double the size of the patch until including enough healthy regions. For the following iterations, we set $\alpha = 1$ and compute D_{SSD} on entire brain regions. This approach improves the coherence of the synthesis as shown in [12]. In Fig. 1 (f)-(g) and (m)-(n), we show inpainted scans for B (a)-(b) and F (h)-(i), respectively.

Now we describe each energy term of $E(\cdot)$ in (2) and then how to optimize it. For the correspondence term E_C, we apply the normalized cross correlation (NCC) distance D_{NCC} between B and F aligned on Ω_C and the cost function masking using posterior probabilities on the pathological regions (PT):

$$E_C(\boldsymbol{f}_{CB}, \boldsymbol{f}_{CF}; B, F, p_B, p_F) \triangleq \int_{\mathbf{x}\in\Omega_C} \left\{1 - p_{B,PT}(\boldsymbol{f}_{CB}(\mathbf{x}))\right\} \cdot \left\{1 - p_{F,PT}(\boldsymbol{f}_{CF}(\mathbf{x}))\right\} \cdot D_{NCC}(B \circ \boldsymbol{f}_{CB}, F \circ \boldsymbol{f}_{CF}, \mathbf{x})\, d\mathbf{x}\,, \quad (5)$$

where $p_{\cdot,PT}$ is a summation of posteriors for tissue types to be excluded in calculating E_C. Before the inpainting stage, we include whole pathological regions in $p_{B,PT}$ and $p_{F,PT}$ to exclude those regions from calculating correspondences. After the inpainting stage, we only include the tumor region (t=TU) in $p_{B,PT}$ and the cavity region (t=CA) in $p_{F,PT}$, so the inpainted regions are used for computing E_C. The pathological term E_P penalizes mismatched regions between posteriors of tumor in B ($p_{B,TU}$) and cavity in F ($p_{F,CA}$):

$$E_P(\boldsymbol{f}_{CB}, \boldsymbol{f}_{CF}; p_B, p_F) \triangleq \int_{\mathbf{x}\in\Omega_C} \left\{p_{B,TU}(\boldsymbol{f}_{CB}(\mathbf{x})) - p_{F,CA}(\boldsymbol{f}_{CF}(\mathbf{x}))\right\}^2 d\mathbf{x}\,. \quad (6)$$

The smoothness term $E_S(\boldsymbol{f}_{CB}, \boldsymbol{f}_{CF})$ is a regularizer based on Tikhonov operator which measures the smoothness of the mappings $\boldsymbol{f}_{CB}$ and $\boldsymbol{f}_{CF}$. To minimize $E(\cdot)$ in (2), we use the discrete-continuous optimization method proposed in [4]. This method updates the initial mapping $\boldsymbol{f}_{BF}^0$ by finding a global solution on the coarse search space through discrete optimization and then refining the solution using continuous optimization.

4 Experiments

We tested our method on a set composed of pre-operative and follow-up MR brain scans of 24 glioma patients. For preprocessing, we co-registered all four modalities (T1, T1-CE, T2, and FLAIR), corrected MR field inhomogeneity, and scaled intensities to fit $[0, 255]$. For all 24 subjects, an expert manually segmented tumor on the pre-operative scan and cavity on the follow-up scan. We computed the Dice score between the tumor region and the cavity region aligned to the pre-operative scan by the method. Also, two experts placed landmarks on the

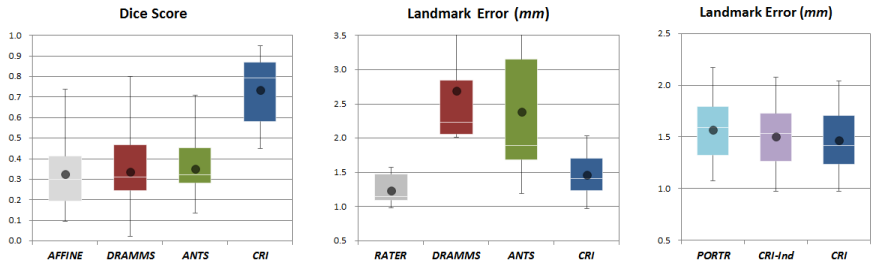

Fig. 2. Box-and-whisker plots of Dice scores on segmentation of pathology (left) and average landmark errors (middle and right). Bars start at the lower quartile and end at the upper quartile with the white line representing the median. Black dots represent the mean errors. *AFFINE* shows the errors of the affine registration and *RATER* denotes the landmark errors of the second rater.

scans of 10 randomly selected subjects. One expert defined 20 landmarks inside 30 mm distance to the tumor boundary on the pre-operative scan. Then both experts independently found corresponding landmarks in the follow-up scan. The landmark error is defined as the mean distance between the landmarks aligned by the method and the corresponding ones set by the expert.

Our method, denoted as *CRI*, requires minimal user inputs including seed point and radius for each tumor and initial mean values for each tissue type for segmenters described in Sec. 2. The correspondence term (5) is only based on T1 and T1-CE as the other two modalities (T2 and FLAIR) decrease the accuracy due to their lower resolutions. We thus applied inpainting on T1 and T1-CE only. For inpainting, we used $N = 64$ T1 healthy brain templates, and applied 10 iterations which is sufficient to create coherent synthesis. We represent *PORTR* as the method runs without inpainting, which corresponds to [4], and *CRI-Ind* as applying independent inpainting by always setting $\alpha = 0$ in (3) and (4). We also applied state-of-the-art registration methods including *DRAMMS* [8] and *ANTS* [2] on our test set. For both methods, we provide the foreground mask to be used for masking out pathological regions.

Fig. 2 (left) shows results on Dice scores for the pathological regions. The average Dice score of *CRI* shows 56%, 54%, and 52% higher than *AFFINE*, *DRAMMS*, and *ANTS*, respectively. *CRI* performed significantly better than the other comparing methods ($p < 0.0001$). Fig. 2 (middle and right) shows results on landmark errors. In the middle figure, *CRI* has the lowest mean error, closest to that of *RATER* and its mean error is 46% lower than *DRAMMS* and 39% lower than *ANTS*. In the right figure, the method using inpainting, *CRI* and *CRI-Ind* performed better than *PORTR* the one without inpainting. The mean error of *CRI* is 7% lower than *PORTR* and 2% lower than *CRI-Ind*. *CRI* performed significantly better than *PORTR* ($p < 0.01$). In Fig. 3, we visually compare the registration results of selected subjects. The aligned follow-up of *CRI* (e) matches better with the pre-operative scan (a) than those of other methods (c)-(d). Also, estimated patient specific templates shown in (f)-(g) shows reasonable restorations of the normal anatomy specific to the scan.

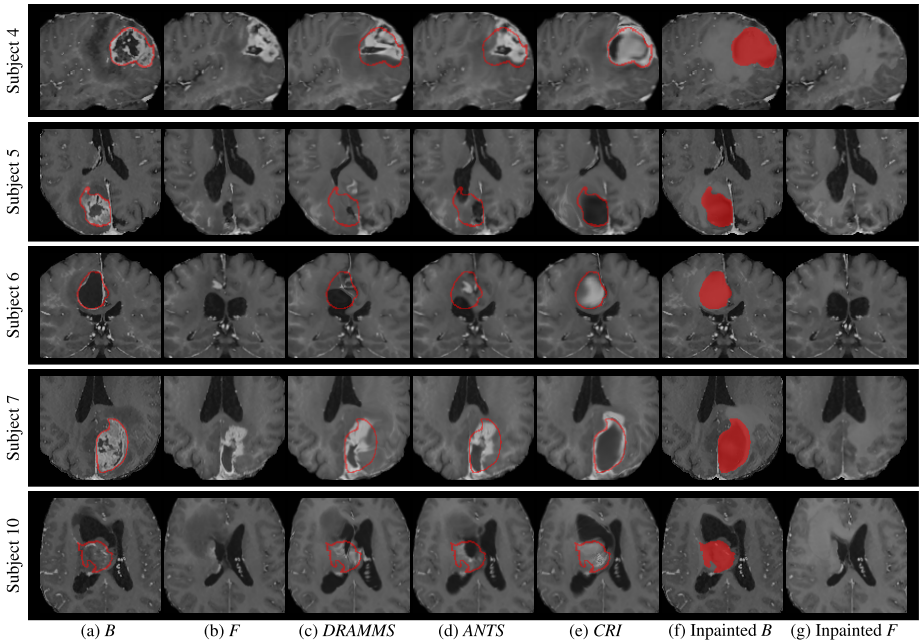

Fig. 3. Registration results for each method. In each row, we show T1-CE images of the pre-operative scan B in (a) and the follow-up scan F in (b). (c)-(e) show the registered F using *DRAMMS*, *ANTS*, and *CRI*, respectively. For B and registered F, boundaries of segmented tumor is overlaid. (f)-(g) show B and F inpainted by *CRI*. In (f), tumor regions are masked as they don't belong to the normal anatomy.

5 Conclusion

In this paper, we proposed a new method combining registration and estimation of patient specific templates for pre-operative and follow-up brain tumor scans. We estimated large deformations on the pre-operative scan using the symmetric registration framework initialized by the joint segmentation-registration which grows a tumor on the atlas aligned on the follow-up scan. The registration on tumor regions of the pre-operative scan was guided to match with cavity on the follow-up scan by the pathological term E_P. To estimate the registration on the entire pathological regions reliably, we estimated patient specific templates by inpainting pathological regions using the patch-based synthesis based on the healthy brain population. Therefore, we were able to explicitly address missing correspondences and inconsistent intensity profile problems. Our method was evaluated on the scans of 24 glioma patients and performed the best among compared registration methods.

Acknowledgement. This work was supported by the National Institutes of Health (NIH) under Grant R01 NS042645.

References

1. Akbari, H., Macyszyn, L., Da, X., Wolf, R.L., Bilello, M., Verma, R., O'Rourke, D.M., Davatzikos, C.: Pattern Analysis of Dynamic Susceptibility Contrast-enhanced MR Imaging Demonstrates Peritumoral Tissue Heterogeneity. Radiology 273(2), 502–510 (2014)
2. Avants, B.B., Epstein, C.L., Grossman, M., Gee, J.C.: Symmetric diffeomorphic image registration with cross-correlation: Evaluating automated labeling of elderly and neurodegenerative brain. Med. Image Anal. 12(1), 26–41 (2008)
3. Chitphakdithai, N., Duncan, J.S.: Non-rigid registration with missing correspondences in preoperative and postresection brain images. In: Jiang, T., Navab, N., Pluim, J.P.W., Viergever, M.A. (eds.) MICCAI 2010, Part I. LNCS, vol. 6361, pp. 367–374. Springer, Heidelberg (2010)
4. Kwon, D., Niethammer, M., Akbari, H., Bilello, M., Davatzikos, C., Pohl, K.M.: PORTR: Pre-Operative and Post-Recurrence Brain Tumor Registration. IEEE Trans. Med. Imaging 33(3), 651–667 (2014)
5. Kwon, D., Shinohara, R.T., Akbari, H., Davatzikos, C.: Combining generative models for multifocal glioma segmentation and registration. In: Golland, P., Hata, N., Barillot, C., Hornegger, J., Howe, R. (eds.) MICCAI 2014, Part I. LNCS, vol. 8673, pp. 763–770. Springer, Heidelberg (2014)
6. Liu, X., Niethammer, M., Kwitt, R., McCormick, M., Aylward, S.R.: Low-rank to the rescue – atlas-based analyses in the presence of pathologies. In: Golland, P., Hata, N., Barillot, C., Hornegger, J., Howe, R. (eds.) MICCAI 2014, Part III. LNCS, vol. 8675, pp. 97–104. Springer, Heidelberg (2014)
7. Niethammer, M., Hart, G.L., Pace, D.F., Vespa, P.M., Irimia, A., Van Horn, J.D., Aylward, S.R.: Geometric metamorphosis. In: Fichtinger, G., Martel, A., Peters, T. (eds.) MICCAI 2011, Part II. LNCS, vol. 6892, pp. 639–646. Springer, Heidelberg (2011)
8. Ou, Y., Sotiras, A., Paragios, N., Davatzikos, C.: DRAMMS: Deformable registration via attribute matching and mutual-saliency weighting. Med. Image Anal. 15(4), 622–639 (2011)
9. Periaswamy, S., Farid, H.: Medical image registration with partial data. Med. Image Anal. 10(3), 452–464 (2006)
10. Roy, S., Carass, A., Prince, J.L.: Magnetic Resonance Image Example-Based Contrast Synthesis. IEEE Trans. Med. Imaging 32(12), 2348–2363 (2013)
11. Sdika, M., Pelletier, D.: Nonrigid registration of multiple sclerosis brain images using lesion inpainting for morphometry or lesion mapping. Hum. Brain Mapp. 30(4), 1060–1067 (2009)
12. Ye, D.H., Zikic, D., Glocker, B., Criminisi, A., Konukoglu, E.: Modality propagation: coherent synthesis of subject-specific scans with data-driven regularization. In: Mori, K., Sakuma, I., Sato, Y., Barillot, C., Navab, N. (eds.) MICCAI 2013, Part I. LNCS, vol. 8149, pp. 606–613. Springer, Heidelberg (2013)